Proceedings World Geothermal Congress 2010
Bali, Indonesia, 25-29 April 2010

Microearthquake Survey at the Buranga Geothermal Prospect, Western Uganda

Norbert Ochmann[1], Michael Kraml[1], Paula Babirye[2] and Michael Lindenfeld[1]

[1]BGR, Federal Institute for Geosciences and Natural Resources, Stilleweg 2, D-30655 Hannover, Germany

[2]GSMD, Geological Survey and Mines Department, P.O. Box 9, Entebbe, Uganda

norbert.ochmann@bgr.de

Keywords: seismicity, gas composition, tomography, drilling location

ABSTRACT

The BGR supports the Government of Uganda in the geoscientific investigations at the Buranga geothermal prospect since 2004. The objective of the project is to raise the knowledge about Buranga to a level (pre-feasibility status) that can be the base for planning of exploration wells.

Geochemical findings, which have been achieved in the framework of the joint project, proofed the existence of a magmatic body that most likely serves as the heat source of the hot springs. Hence the task of active ground geophysics was detecting and delineating this magmatic intrusion. The known high seismicity (about 500 local earthquakes per month) suggested that Buranga provides excellent requirements to apply seismology.

4185 earthquakes have been localized in the period January to August 2006 with 15 stations. This huge data set was suitable to apply an inversion method called seismological tomography. The results of the tomography clearly reveal definite low velocity anomalies in the subsurface. The strongest P-wave velocity anomaly (-9 %) in 10 km depth is located directly south of the Buranga hot springs. Taking the findings of geochemistry into account, the most plausible conclusion for the observed velocity reductions are high temperature anomalies. These temperature anomalies could be a result of a hot actively degassing magma intrusion, which is the heat source for the hot springs.

By combining all findings a conceptual model for the Buranga geothermal prospect was developed and on the basis of this model a possible drilling location was suggested. Assuming favourable conditions a decentralized ORC power plant might be feasible in this area.

1. INTRODUCTION

With climate protection and sustainable development of natural resources as objectives, the German government has initiated a program for the support of renewable energy projects, specifically within the scope of Technical Cooperation. Within the framework of this program, the GEOTHERM subprogram for the support of geothermal energy projects was begun in early 2003, implemented by BGR (German Geological Survey).

The objective of the program is to promote the use of geothermal energy in partner countries by kicking off development at promising sites. The program supports partner countries worldwide, preferably in areas with high geothermal potential. The aim is to minimize the high initial investment risk associated with the development of geothermal resources.

In Uganda power generation is dominated by hydropower. Uganda has a total generating electricity capacity of 397 MW (2004), mainly generated by a single source on the River Nile (380 MW), the rest by few small hydropower plants. The electrification rate is very low, with grid access of only 9% for the whole country and 3% in rural areas. Additional 1% of the population provides itself with electricity using generators, car batteries and solar PV systems. The electricity demand is estimated to be growing at a rate of 7-8% per annum resulting in a need for an increasing power generation.

The Government of Uganda is studying ways to meet the increasing energy demand by other indigenous energy sources. Geothermal energy presents a high priority alternative to hydropower. Uganda's potential for geothermal power generation is estimated at about 450 MW. The most promising geothermal areas are Buranga, Katwe and Kibiro (Bahati et al., 2005) which are situated in West-Uganda in the Albertine Rift, a part of the western branch of the East African Rift System.

Since the end of 2004 BGR, through the GEOTHERM program, supports the Government of Uganda in the geoscientific investigations at the Buranga geothermal prospect. The objective of the project is to raise the knowledge about Buranga to a level (pre-feasibility status) that can be the base for planning of exploration wells. The Ugandan project partner is the Geological Survey and Mines Department (GSMD).

2. SURVEY AREA

The Buranga hot springs are situated in the Albertine Rift (western branch of the East African Rift) in the Semliki National Park in Bundibugyo district to the west of the Rwenzori Massif. The national park extends to the north and west to the Semliki River, which is the borderline to the Democratic Republic of Congo. The springs are situated in a swamp in the tropical rain forest a few hundred meters westerly of the Bwamba fault, which forms the western flank of the Rwenzori and the eastern scarp of the rift respectively. At the Bwamba fault the Precambrian basement rocks of the Rwenzori Massif dip 60-65° west and strike 20-40° NNE. The Buranga hot springs consist of 37 springs with an overall flow rate of 30 l/s and temperatures up to 98.4°C.

Figure 1:The largest spring of the Buranga hot springs has deposited large amounts of travertine

The survey area is located in a terrain that is very difficult to access. The eastern part of the study area is situated at the steeply dipping escarpment of the Rwenzori Massif (Bwamba fault). The western part of the survey area is covered by dense tropical rain forest with creeks and swamps. The hot springs are located in a swampy terrain in clearings of the rain forest. In the northern part of the survey area the rain forest is thinning out and the terrain changes to a plain covered by grass.

3. PREVIOUS WORK

In 1953/54 the Geological Survey of Uganda carried out a drilling program at Buranga to determine if geothermal power could be developed. Three boreholes were drilled in Buranga with depths up to 349 m (Árnason, 2003). One Borehole, No. 3 produced thermal water that is still flowing; in February 2005 the measured water temperature was 62°C.

In 1973 two Schlumberger soundings were measured at Buranga. The soundings show that the resistivities of the rift sediments decrease towards the hot springs and that the high resistive basement dips west at the Bwamba fault.

Pallister (1952) and Árnason (2003) consider that geothermal activity of the Buranga hot springs is most likely related to tectonic activity in the rift. It was observed that historical earthquakes, e.g. 20th March 1966, 17th May 1966 (both magnitude 6.1-6.3, epicenters about 30 km SW of Buranga) and 6th February 1994 incl. some after quakes (magnitude 6.3, epicenter south of Fort Portal), changed the geothermal activity of the Buranga hot springs. After the latter earthquake a new group of hot springs opened at Buranga (Gislason et al., 1994) which shows that seismological activity can open or reactivate flow paths for thermal water in the basements and sediments.

The observation that after strong earthquakes local displacements of the hot springs as well as changes of the individual flow rates had occurred suggests that the activity of the Buranga hot springs is very much related to an active fault system and that these tectonically active faults might provide the migration paths for the hydrothermal water.

Chemical analysis and geothermometry of water samples from hot springs in Buranga indicated reservoir temperatures of about 120°C, with a possible maximum of 150°C (Ármannsson, 1994). Recent isotope geothermometry indicated temperatures of 200°C (IAEA, 2003).

The GSMD compiled a soil temperature map of Buranga. The soil temperature was measured at constant depth (several centimeters) on profiles which cover most part of the area of the hot springs. The map shows a high temperature anomaly that strikes in SE-NW direction. The anomaly passes the area where the hottest spring is located and the new group of hot springs opened after the earthquake from 6th February 1994.

A detailed summary of results of previous geoscientific investigations can be found in Árnason (1994) and Árnason (2003).

4. STUDIES WITHIN BGR/GSMD PROJECT

The geoscientific studies of the joint BGR/GSMD project were aimed at achieving and solving the following objectives and questions: clarification of the origin of the thermal water of the Buranga hot springs, validation or disproof of the existence of a magmatic heat source and in the first case its localization, detection of faults/fractures under the sedimentary cover where thermal waters may flow up, mapping the extent of thermal waters in the rift at Buranga prospect and localization of active faults in the region around Buranga.

Several ideas for conceptual models of the Buranga geothermal prospect existed:

• Buranga is fed by basinal brines (“oilfield brines”) of the rift: Sedimentary brines from the Tertiary sedimentary rocks in the rift in depth >2 km below the surface of Buranga with temperatures >125°C stream up along Bwamba fault (overpressure of sedimentary brines, density driven)

• Buranga is fed by meteoric fluids from high Rwenzori Mountains: Meteoric water flows in open faults down from the higher part of the Rwenzori Massif (3.000-5.000 m asl), and is heated in a depth of 2.000 m below surface (normal geothermal gradient), upstream along Bwamba fault (density driven)

• Buranga is fed by magmatic fluids of a hidden magma chamber together with meteoric fluids of Rwenzori: Active magmatic intrusion below Buranga which is also the source of heat and gases

The joint BGR/GSMD project started with the aim to validate or disprove the existing conceptual models or to develop a better one. To achieve this, a cooperation of various geoscientific departments (structural geology, geochemistry and geophysics) commenced.

A volcanic field is found east of the Rwenzori Massif close to Fort Portal. At Lake Albert indications for magmatic intrusions were deduced from aeromagnetic investigations. In the region of the Albertine Rift, where Buranga is located, no geological surface indications for volcanic activity or intrusive dikes were found so far which could act as a heat source for the thermal water.

However, from carbon isotopic composition of CO_2 a first indication of a mantle source for the gas released at Buranga hot springs was found. This was confirmed by He isotopic analyses indicating a contribution of >30% mantle He. These findings imply that a still hot actively degassing magma body exists in the subsurface of Buranga area. The magma body was so far not detected by aeromagnetic surveys perhaps due to its presumed location at or within

the Rwenzori basement rocks and its still hot temperature (Kraml & Kato, 2006).

The fact that geochemical results proofed the existence of a magmatic body in Buranga area suggests itself to serve as the heat source of the hot springs. This finding defined the task of active ground geophysics in detecting and delineating the magmatic intrusion and recommending locations for geothermal exploration boreholes.

In the beginning of 2005 BGR started a first attempt with DC-Soundings, TEM and Gravity (Stadtler & Kraml, 2005). These methods were carried out as far as possible, but results of this survey were insufficient to delineate a geothermal reservoir for two reasons:

- The avoided to cover adequately the survey area with the measurements necessary for identifying a potential geothermal reservoir. Measurements could only be carried out in a small strip along the Rwenzori Massif.
- Low resistivities in the subsurface were detected almost everywhere leading to insufficient distinction of results between geothermal active and non-active areas. bad/impossible accessibility of the terrain

The known high seismicity (about 500 local earthquakes per month) suggested that Buranga provides excellent requirements to apply seismology. The observation that the activity of the Buranga hot springs is very much related to an active fault system and that these tectonically active faults might provide the migration paths for the hydrothermal water suggested seismology as the appropriate method to be applied in Buranga.

4.1 Known Trends in Seismicity in Rwenzori Area

The main trends in seismicity of the western part of the East African rift system are fairly clear from previous studies, which used teleseismic stations (e.g., DeBremaeker. 1959; Sykes and Landisman, 1964; Wohlenberg, 1969; Fairhead and Girdler, 1971). For better understanding the structure and development of the Rwenzori Mountain region of the East African rift system Maasha (1975) carried out a microearthquake survey for a three month period in 1973 with four portable seismographs.

He found that the Rwenzori Region is the most seismically active area in Uganda. In the Rwenzori Region the spatial trends of the microearthquakes are correlated with the major rift faults and volcanic zones on the eastern side of the Rwenzori mountains. The seismicity is shown to extend beneath and transverse to the Rwenzori Mountain block, with hypocentral depths ranged between 0 and 40 km. Elsewhere in the studied region, composite focal mechanism solutions show dip slip motion along steeply dipping planes (Bwamba, Ruimi-Wasa, and Nyamwamba faults). The extensional axes trend east-west. The motion tends to raise the mountain block relative to the surrounding country. A foca1 mechanism determined at the junction of the northern and southern Rwenzori indicates that the northern portion is being uplifted with respect to the southern block.

5. FEATURES OF THE LOCAL SEISMICITY

Deployment of seismological equipment in Buranga region to record local earthquakes was started in May 2005 with three seismological stations only. By and by the number was increased to 15 stations. Fig. 2 shows the final state of the seismological network that was operated from January 2006 until August, 2006.

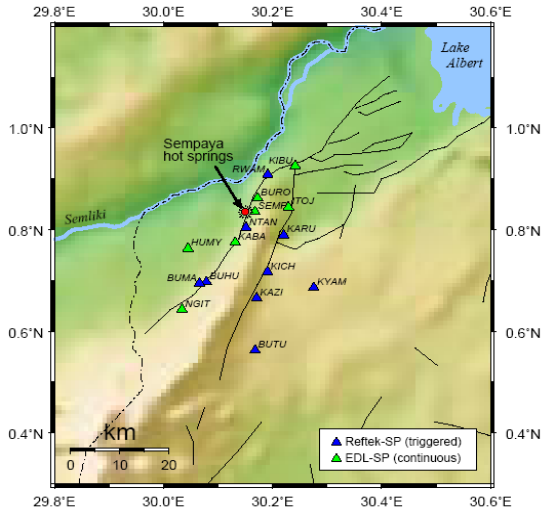

Figure 2: Map showing the distribution of stations (triangles). Black lines close to the triangles are the marginal faults of the Rwenzori Mountains

In 2005 only Reftek equipment (kindly provided by GFZ Potsdam) was available for the project which was operated in triggered mode. In 2006 seven more Earth Data Logger (EDL in cooperation with RiftLink project, www.riftlink.de) were deployed and operated in continuous mode. Short period 1 Hz seismometers of type Mark L-4 3D (kindly provided by Geophysical Institute of FU Berlin) had been used at every station.

HYPOCENTER (Lienert et al., 1986; Lienert & Havskov, 1995) was used for hypocenter localization. In total, 49721 phase readings (P- and S-wave arrival times), corresponding to 4185 events, had been picked manually. The 1-D velocity model for the initial determination of hypocenters is given in Table 1. P-velocities are slightly faster than those of the IASPEI standard earth model (Kennett, 1991). A constant P/S-velocity ratio of 1.74 is assumed. While the 1-D velocity model gives a first impression of the location of hypocenters, it certainly represents the true velocity variations insufficiently. Seismic event locations based on regional 1-D velocity-depth sections can have bias errors caused by travel-time variations within different tectonic provinces and due to ray-paths crossing boundaries between tectonic provinces with different crustal and upper mantle velocity structures.

Table 1. Velocity Model Used for the Initial Determination of Hypocenters.

Depth [km]	Vp [km/s]	Vs [km/s]
0.	6.2	3.6
12.	6.6	3.8
23.	7.1	4.1
31.	8.05	4.63
50.	8.25	4.71
80.	8.5	4.9

The Rwenzori mountain range is characterized by gneisses of relatively high velocity, whereas the neighbouring regions to North and West are characterized by slower velocities due to sedimentary layers in the rift (Schlüter, 2006). A velocity model with relatively high values of P-wave velocity (6.2 km/s) close to the surface was used for the localization of hypocenters. While this 1-D model probably represents a valid approximation for the eastern section of the region of interest, the velocities in the western section are likely overestimated. It is noted here, that a highly improved localization of the seismic events as well as a 3-D velocity model will result from the application of the tomographic inversion. Tests reveal that moderate changes of the initial velocity model do not have significant effects of the results of the 3-D tomographic velocity inversion described below.

5.1 Localization Results

Figure 3 shows locations of earthquakes that have been recorded during the above mentioned operation period of the network. The stations are marked as triangles. The majority of events exhibits focal depths between 10 and 30 km; the deepest events occur at depths of about 55 km.

For most events, the error of localizations is in the order of about 2-3 km. 80% of all hypocenters exhibit localization errors that are smaller than 5 km. The source-time error for most events is smaller than 0.4 sec. About 80 % of events exhibit a source time error smaller than 0.8 sec.

Obviously, few earthquakes occur within the northern part of the Rwenzori block; most events occur outside of the surface expressions of the main marginal faults, the Bwamba fault (west) and the Ruimi-Wasa fault (east), as indicated by the black solid lines in Figure 2 and 3.

Events lining the flanks of the Rwenzori range are connected by earthquakes along an east-west trending line near 0.6N, thus separating the northern and southern blocks of the Rwenzori range. This is in agreement with observations by Maasha (1975b). Further to the south, most earthquakes are located to the east of the mountains.

From Figure 3, there is no obvious strong correlation between the surface expressions of known faults and epicentre locations. The events seem to be arranged in clustered form and relatively diffuse rather than along linear structures. In part this may be due to the relatively large error ($\approx \pm$ 3 km) in locating events which occur outside of the array of stations. However, before a more detailed analysis of hypocenters can take place the tomographic inversion of the travel-time residuals and the derivation of a 3-D velocity model should be discussed.

5.2 Iversion of Travel Time Data

In general, the microearthquake activity around Rwenzori was observed to provide information on the question whether an assumed magmatic intrusion could be detected with this approach or not. The conception might be explained with the following sketch:

Let us assume a homogeneous crust in which an earthquake happens. Some of the waves that travel to the recording sites at the surface traverse a magmatic intrusion. Let us also assume that this intrusion body has a different velocity from the homogeneous crust. If we correct the travel time for the distance covered, the rays that passed the anomaly will arrive the sites late or early depending on the body's velocity being low or high. The early or late arrivals are usually called travel time residuals. These travel time residuals are used to calculate the involved velocity perturbations.

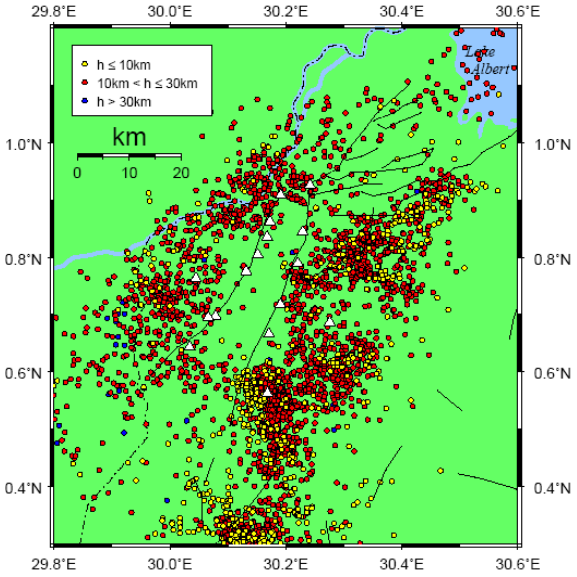

Figure 3: Location of 4185 local earthquakes. Recording stations are marked as triangles. Different colors of epicenters indicate different focal depths

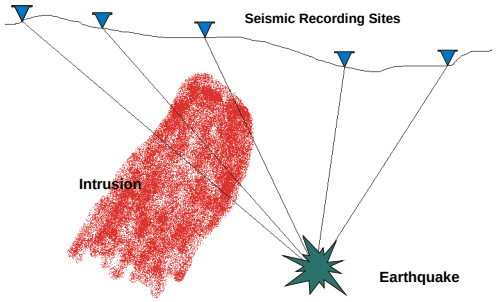

Figure 4: Seismic rays traveling from an earthquake source to recording sites at the surface can exhibit early or late arrival times depending on the velocity anomalies they have passed.

The target of the procedure is to minimize travel time residuals of P- and S-waves at the recording sites. The final solution is achieved using an iterative procedure for earthquake relocation and simultaneous determination of the velocity structure.

5.3 Results of the Tomography

A tomographic inversion of the travel-time data was performed to determine the three-dimensional (3-D) structure of the P-and S-wave velocity of the crust beneath the network of stations. The method of travel-time inversion for local earthquakes used here is based on recent developments by Koulakov & Sobolev (2006) and Yakovlev et al. (2007).

The initial velocity model for the tomographic inversion is the same as the 1-D velocity model used for the preliminary

localization of hypocenters (Table 1). A total number of 2051 events were included in the inversion. This is about half of the total number of events (4185) recorded and identified during the operation of the network. The reduction results in part from the requirement that only those events are used for the inversion for which at least 8 phase readings were determined. This means that each event was recorded by at least 4 stations if both, P and S-wave arrival times were identified. The inversion includes 28644 rays (14445 P-rays and 14199 S-rays) resulting in an average number of about 14 phase readings per event. A further requirement is that the distance between the epicentre and the centre of the array should be less than about 110 km. This is to exclude distant events for which the localization error is relatively large.

In the course of the tomographic inversion (during each step of the iteration) a 3-D velocity model is derived first. Then, on the basis of the improved velocity model, the earthquake hypocenters are re-calculated. The iteration procedure ends when the difference between the new and the previous results becomes insignificant.

In Figure 5 the position of hypocenters after re-localization is shown. One obvious effect of the re-localization is the stronger clustering of events near, for example, station BUTU or northeast of station KYAM. Events to the west of the Rwenzori range have shifted slightly to the west, now following the course of the Semliki river more closely. This may indicate that the river itself follows partly the surface expression of an active fault. After re-localization, there exists an almost aseismic area to the west of stations SEMP, NTAN, KABA - close to the location of the hot springs. Furthermore, shallow and deep events near station BUTU are more consistently separated after re-localization. This indicates that these events correspond to a dipping active fault plane, striking north-south.

5.4 Analysis of the Velocity Structure

Figure 5 presents the data subset that was used for the tomographic inversion. The vertical sections help to imaging the dense ray coverage inside the investigation area.

Generally the P-wave results may be considered more reliable due to larger uncertainties in the determination of S-wave arrival times. Therefore, the P-wave results are basically discussed. The S-wave results can be found in Rümpker et al. (2007). The tomographic inversion results in refined earthquake locations as well as in 3-D velocity perturbations with respect to the initial 1-D model. Examples for horizontal sections of P-wave velocity anomalies at a depth of 1 to 20 km are given in Figure 6. Detailed results for additional depths and for P- and S-wave anomalies are given in Rümpker et al. (2007).

Low velocity anomalies are visible at all depths levels. They are relatively strong at shallow depth (1-5 km) and are arranged close to the Bwamba fault, the margin of the Rwenzori Mountains. At shallow depth they are outside of the Rwenzori block. Their position does not coincide with the hot springs; they are not directly beneath them. At shallow depth (1-3 km) the results show that a large low-velocity anomaly exists in the north-western section of the region under investigation. It is interesting to note that the Buranga hot springs are located at the boundary of this anomaly at the transition between slow and fast regions. The low-velocity anomaly broadens at greater depths (> 5 km). This is similarly seen in the vertical tomographic sections shown in Fig. 7. The faster velocities to the east of the hot springs are located beneath the northern block of the Rwenzori range.

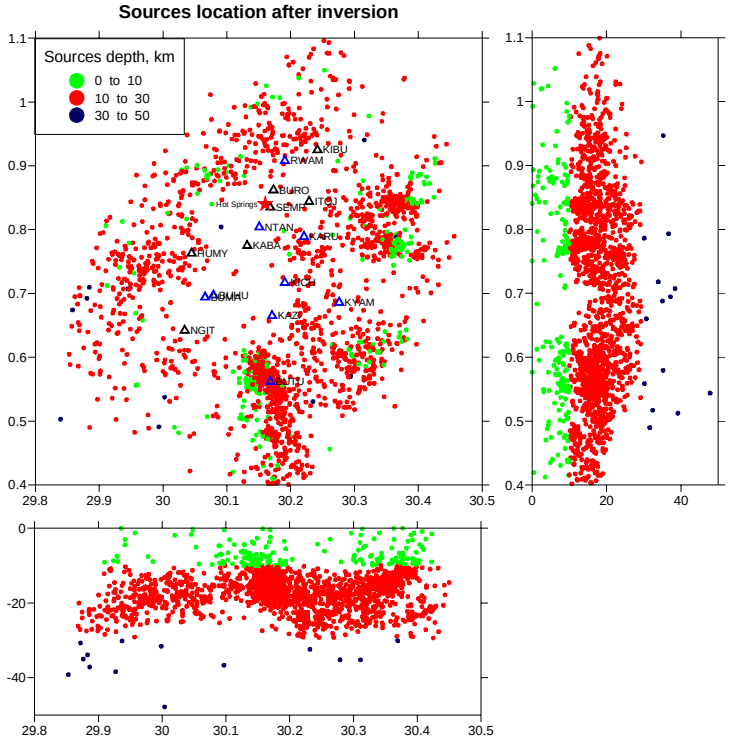

Figure 5: A data subset of 2051 events was used for an inversion meaning a total number of 28644 P- and S-rays passed the investigated area. The vertical sections (upper right and lower left) present a projection of focal depths

At greater depth low velocity anomalies are still observable but their position was dislocated towards the centre of the Rwenzori block. The anomalies are as strong as at shallower level. A smaller, well resolved low-velocity anomaly is found near the eastern station of KARU (see Fig. 2 or 5). The anomalies appear to remain separated down to a depth of about 7.5 km. To the south some additional individual anomalies can be found. They merge to a large, more centrally-located, low-velocity anomaly at a depth of about 10 km.

In relation to the location of the hot springs there are several interesting observations that can be derived from this survey. The hot springs are located above the boundary between relatively slow and fast regions

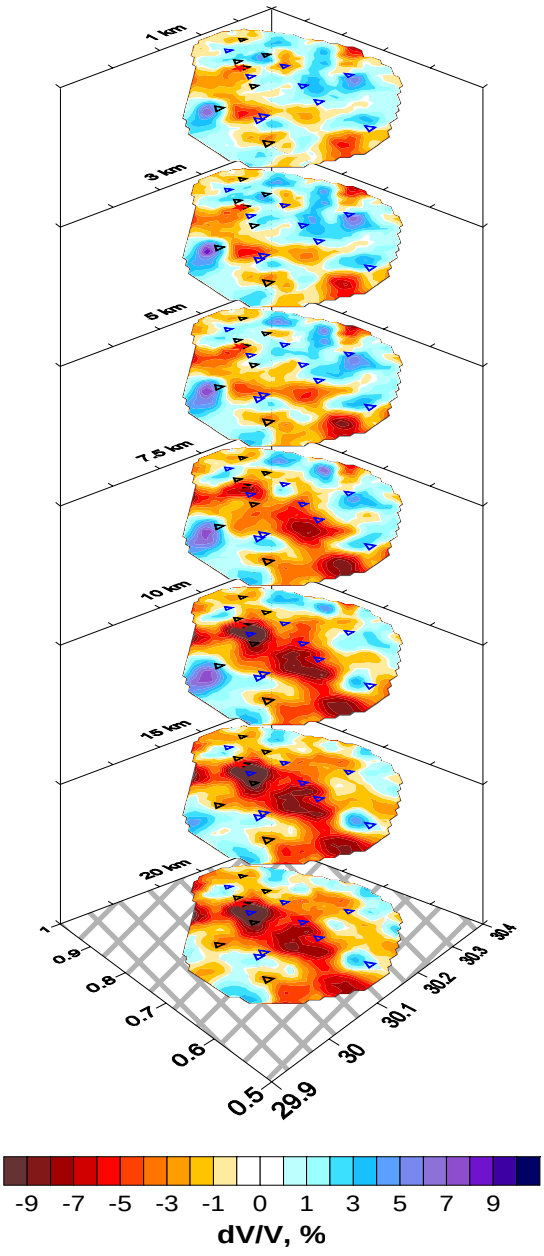

Figure 6: The anomalies of P- and S-velocities may be presented in horizontal sections in different depth levels (here only for P). The assumed "hot" magmatic intrusion should figure out as negative velocity anomaly

In the crust at depth range between 0 and 7 km. The low velocity anomaly broadens beneath this depth range and connects with other smaller anomalies to the east and south. Also, the region to the west/south-west of the hot springs is almost aseismic and it coincides with a low velocity anomaly in the crust (Fig. 6 and Fig. 7).

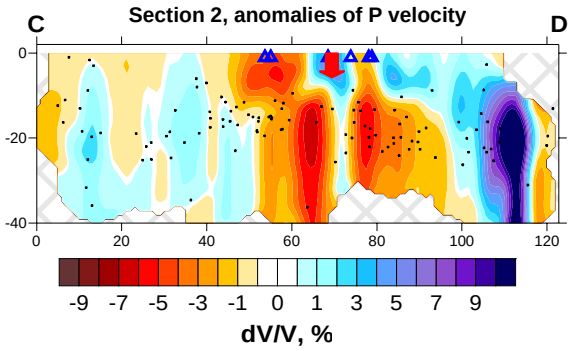

Figure 7: The anomalies of P- and S-velocities may also be presented in vertical sections (here only for P). This section follows the direction of Bwamba fault (western Rwenzori margin). The position of the hot springs is marked with arrow, C belongs to southern direction, D is northeast

Absolute velocities are difficult to estimate from tomographic inversions, as true maximum amplitudes of the anomalies are usually underestimated. Based upon the results from geochemistry the velocity anomalies in the subsurface are certainly caused by temperature effects but its impact on P- and S-wave velocities is difficult to derive. After Kern (1978) and Landolt-Börnstein (1982) the velocity reduction may be estimated at about 0.1 km/s per 100°C. Accordingly a 10 % anomaly corresponds to about 0.7 km/s variation in P-wave velocity and 0.4 km/s change in S-wave velocity.

CONCLUSIONS

The survey area at the Buranga geothermal prospect is only partly accessible because of the terrain conditions with the steeply dipping escarpment of the Rwenzori Massif and dense tropical rain forest with creeks and swamps. Due to these conditions, the ground geophysical measurements (resistivity and gravity) of the field survey in February/March 2005 were restricted to a small zone along the Rwenzori Massif.

However, the resistivity methods (Schlumberger soundings, dipole/dipole-mapping and TEM soundings), which are not presented here, result in a consistent model showing the resistivity along the Bwamba fault. In the vicinity of the hot springs a high conductive anomaly was located which extends over about 2.5 km in north-south direction in the rift along the escarpment of the Rwenzori Massif. The anomaly is probably caused by thermal water which has infiltrated the rift sediments. This is consistent with chemical analyses which had been taken at old boreholes (e.g. No.3 in section 3). Thermal water has also infiltrated the rift sediments north of the Buranga hot springs in the northern part of the survey area. This observation is supported by the fluid chemistry of other hydrogeological watersamples.

The seismological results revealed that in the subsurface of the Rwenzori region large, strong velocity anomalies exists which reduce significantly the local velocity of seismic waves. Taking into account that isotope geochemical results

clearly proved that mantle helium and volcanic CO_2 are released at Buranga hot springs, it is most likely that the reduction in velocity is due to high temperature anomalies. These temperature anomalies are the result of a hot, actively degassing magma intrusion, which also is the heat source of the hot springs.

The strongest P-wave velocity anomaly (-9 %) in 10 km depth is located directly south of the Buranga hot springs (Fig. 8). The centre of the anomaly is situated below the escarpment of the Bwamba fault. If its dip of about 60°W continues in depth, it can be assumed that the centre of the anomaly lies within the Precambrian basement. The low velocity anomaly coincides with the aseismic region which could be a further indication that the reduction in velocity is caused by temperature effects in the subsurface of this region. High temperatures would not allow rocks to develop stress levels that are high enough to be released as earthquakes (ductile behaviour).

The size of the low velocity anomalies is in the same order as the magmatic intrusives which were interpreted from aeromagnetic data in the subsurface of Lake Albert and Lake Edward. However, it has to be noted that general difficulties exist to separate the effects of temperature-related velocity reductions from those related to changes in rock type, i.e. the sedimentary infill of the rift in shallow depth levels.

Because of the clear indications for an active magmatic intrusion which could serve as heat source for the hydrothermal system in the subsurface of the Buranga geothermal prospect, a magmatic body was included in the conceptual model (Fig. 9). The model is integrated in a 3-D satellite image as vertical section along the Bwamba fault. It has to be considered that the section is vertical, although the fault has a dipping angle (ca. 60°W at Buranga).

The recharge area for the thermal water, which emanates at the Buranga hot springs, is located in the high Rwenzori region (proven by isotope hydrological investigation). The meteoric water is descending in the subsurface and flowing towards Buranga most likely along the Bwamba fault. The missing tritium in the thermal water of Buranga (IAEA 2003) indicates a long flow path. The higher temperatures in the subsurface of Buranga, caused by the magmatic intrusion, additionally heats up the meteoric water, which is then forced to rise along the Bwamba fault and the identified transverse fault cutting the rift sediments. The thermal water emanates with temperatures of up to 98°C at the Buranga hot springs which are located within the rift sediments. The convectively rising fluid takes only a short way through the sediments in the upper depth level (mainly through fractures) because the source of salinity is according to chemical data mainly water-rock-interaction with basement rocks but not with sediments.

Furthermore,.it can be concluded that the thermal water has partly infiltrated the rift sediments and formed a local shallow reservoir (interpreted after resistivity measurements) with maximum temperatures around 120°C as e.g. indicated by the fast equilibrating SiO_2 geothermometer. This water is tapped by borehole No.3 which does not reach the Precambrian basement. The low outflow of the borehole is however mixed with cold surface water (=> reduced temperature of around 60°C and reduced salinity compared to Buranga hot springs) as evidenced by much higher discharge rates in the rainy seasons. The fluids discharging at Buranga hot springs do not show significant seasonal variations in flow rate because the geothermal system is fault controlled and recharged continuously from far distance (small variations in precipitation in high Rwenzori region).

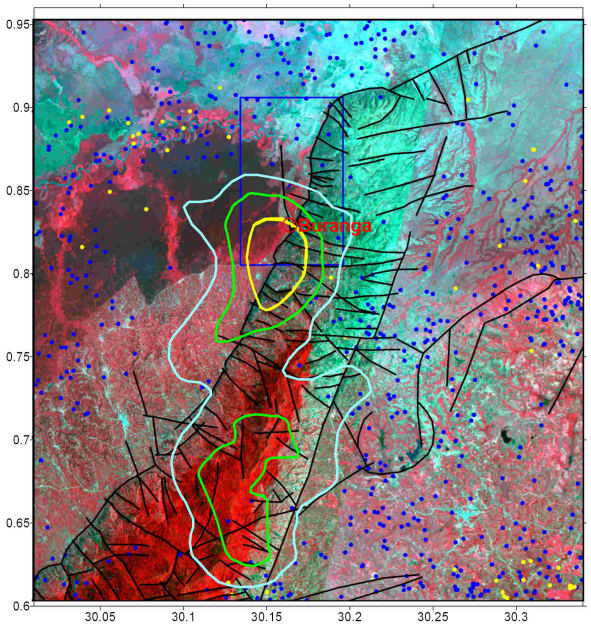

Figure 8: Northern part of a ASTER Satellite image of the Rwenzori Massif, overlain by the lineament pattern and anomalies of P-velocities in 10 km depth (Fig. 6) derived from seismic tomography (light-blue: -3 % dV/V, green: -6 %, yellow: -9 %). Dots represent relocated epicentres; different colours indicate different focal depth (Fig. 5)

The reservoir temperatures estimated from solute, gas and isotopic geothermometers cover a broad temperature range between about 110-210°C. Additionally to the local shallow reservoir at Buranga, it could be concluded that higher temperatures in the subsurface south of Buranga (upflow zone) could be expected, probably around 160°C, because of the proven existence of a heat source for the thermal water which emanates at the Buranga hot springs. This temperature would be sufficient for power generation with binary technology at the Buranga geothermal prospect if the flow rate that is encountered in the borehole is high enough.

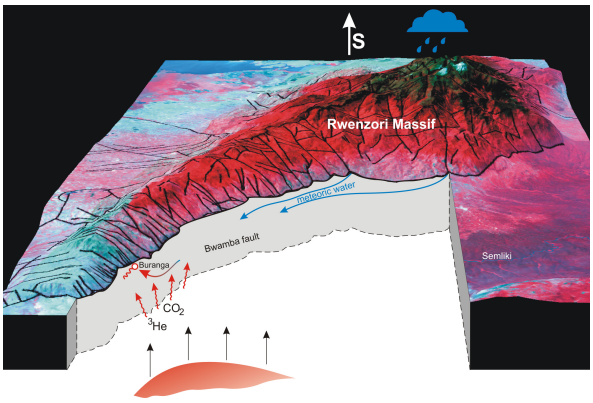

Figure 9: A 3-dimensional view of the Rwenzori Massif from space as seen from the North overlain by a lineament pattern and integrated conceptual model (vertical section along the Bwamba fault) of the Buranga geothermal prospect (not to scale)

The promising project results suggest that the Buranga geothermal prospect is appropriate for further development of a geothermal power plant. The amount and quality of existing geoscientific data allowed a characterisation of the Buranga geothermal system. A possible drilling location should be located within the projected zone of major velocity reduction found in all tomographic inversions (yellow contour in Fig. 8). In combination with the geochemical results this zone is interpreted as the major heat source in the investigated area.

According to the hydrological/hydrochemical results the Bwamba Fault is the major pathway for the geothermal fluids. Therefore the Bwamba Fault is the drilling target. To enhance the chances to encounter zones of highest permeability the drilling location should be at the intersection of Bwamba- and perpendicular faults known from structural interpretation (Fig. 8).

REFERENCES

Ármannsson, H. 1994. Geochemical Studies on Three Geothermal Areas in West and Southwest Uganda. Final report. Geothermal Exploration UGA/92/002, UNDEST/GSMD report

Árnason, K. 1994. Recommendations for Geophysical Studies on Three Geothermal Areas in West and South-West Uganda. Report under the project Geothermal Exploration UGA/92/002, UNDEST/GSMD

Árnason, K. 2003. Geothermal exploration in the Buranga geothermal field in West Uganda. Island Geosurvey, ISOR, Report

Bahati, G. 2003. Geothermal energy in Uganda, country update. International Geothermal Conference, Reykjavik, 2003, 48-53

Bahati, G. & Ármannsson, H. 1995. The chemistry of waters in the Buranga and Kibiro geothermal fields, West Uganda. In: Water-Rock Interaction by Y. K. Kharaka and O.V. Chudaev, A.A.Balkema/Rotterdam/Brookfield/1995

Bahati, G., Pang, Z., Armannsson, H., Isabirye, E.W. & Kato, V. 2005. Hydrology and reservoir characteristics of three geothermal systems in western Uganda. Geothermics, 34, 568-591

DeBremaeker, J. 1959. Seismicity of the West African rift valley, J. Geophys. Res., 64, 1961-1966

Dozith, A. & Mugisha, F. 2004. Structural Analysis of the Albertine Graben Western Uganda. Petroleum Exploration and Production Department, Uganda. Abstract in Proceedings, The East African Rift System: Development, Evolution and Resources, Addis Ababa, Ethiopia, 20.-24. June 2004

Fairhead, J.D., & Girdler, R.W. 1971. The seismicity of Africa, Geophys. J. Roy. Astron. Soc., 24, 271

Gíslason, G., Ngobi, G., Isabirye, E. & Tumwebaze, S. 1994. An Inventory of Three Geothermal Areas in West and Southwest Uganda. Geothermal Exploration UGA/92/002, UNDEST/GSMD, a draft report

IAEA 2003. Isotope hydrology for exploring geothermal resources. IAEA TC-Project, UGA/8/003, Terminal Report

Kennett, B.L.N. (Ed.) 1991. IASPEI 1991 Seismological Tables. Research School of Earth Sciences, Australian National University

Kern, H. 1978 The effect of high temperature and high confining pressure on compressional wave velocities in Quartz-bearing and Quartz-free igneous and metamorphic rocks. Tectonophysics, 44, 185-203

Koulakov, I., & Sobolev, S.V. 2006. Moho depth and three-dimensional P and S structure of the crust and uppermost mantle in the Eastern Mediterranean and Middle East derived from tomographic inversion of local ISC data. Geophysical Journal International, 164, 1, 218-235

Landolt-Börnstein 1982. Zahlenwerte und Funktionen aus Naturwissenschaft und Technik. Springer Verlag

Lienert, B.R.E., Berg, E. & Frazer, L.N. 1986. Hyocenter: An earthquake location method using centered, scaled, and adaptively least squares. BSSA, 76, 771-783

Lienert, B.R.E. & Havskov, J. 1995. A computer program for locating earthquakes both locally and globally. Seismological Research Letters, 66, 26-36

Maasha, N. 1975a. Electrical resistivity and microearthquake surveys of the Sempaya, Lake Kitagata, and Kitagata geothermal anomalies, Western Uganda. Proceedings Second United Nations Symposium on the Development and Use of Geothermal Resources, San Francisco, 20.-29. May 1975, 1103-1112

Maasha, N. 1975b. The Seismicity of the Rwenzori Region in Uganda. Journal of Geophysical Research, 80 (11), 1485-1496

McConnell, R.B. & Brown, J.N. 1954. Drilling for geothermal power at Buranga Hot Springs, Toro. First Progress Report. Geological Survey of Uganda, Unpub. report No. JMB/17 (RBM/16)

Mogi, K. 1967. Earthquakes and fractures. Tectonopysics, 5, 35-55

Ochmann, N., Hollnack, D. & Wohlenberg, J. 1989. Seismological Exploration of the Milos Geothermal Reservoir, Greece. Geothermics, 18, 4, 563-567

Pallister, J. W. 1952. Buranga Hot Springs, Toro, Uganda. Geological Survey of Uganda. Unpub. report No. JWP/14

Pallister J.W. 1954. Drilling for geothermal power at Buranga Hot Springs, Toro; Second Progress Report. Geological Survey of Uganda, Report No. JWP/26

Rümpker, G., Lindenfeld, M. & Yakovlev, A. 2007. Seismological data analysis, earthquake localization and travel-time tomography. GEOTHERM Project: Detailed surface analysis of the Buranga geothermal prospect, West-Uganda. Report, University of Frankfurt

Schlüter, T. 2006. Geological Atlas of Africa. Springer-Verlag Berlin Heidelberg

Stadtler, C. & Kraml, M. 2005. Geophysical and geochemical investigations at the Buranga hot springs, Albertine Rift, Uganda. GEOTHERM Project: Detailed surface analysis of the Buranga geothermal prospect, West-Uganda. Interim Report, Hannover, BGR, 0125802

Sykes, L. R. & Landisman, M. 1964. The seismicity of East Africa, the Gulf of Aden and the Arabian and Red seas. Bull. Seismol. Soc. Amer., 54, 1927-1940

Wohlenberg, J. 1969. Remarks on the seismicity of East Africa between 4°N-12°S and 23°E-40°E. Tectonophysics, 8, 567-577

Yakovlev, A.V., Koulakov, I.Yu. & Tychkov S.A. 2007. Moho depths and three-dimensional velocity structure of the crust and upper mantle beneath the Baikal region, from local tomography. Russian Geology and Geophysics, 48 (2), 204-220